Batteries

DOI: 10.1002/anie.201403734

Use of Graphite as a Highly Reversible Electrode with Superior Cycle Life for Sodium-Ion Batteries by Making Use of Co-Intercalation Phenomena**

*Birte Jache and Philipp Adelhelm**

Abstract: *Although being the standard anode material in lithium-ion batteries (LIBs), graphite so far is considered to fail application in sodium-ion batteries (NIBs) because the Na-C system lacks suitable binary intercalation compounds. Here we show that this limitation can be circumvented by using co-intercalation phenomena in a diglyme-based electrolyte. The resulting compound is a stage-I ternary intercalation compound with an estimated stoichiometry of $Na(diglyme)_2C_{20}$. Highlights of the electrode reaction are its high energy efficiency, the small irreversible loss during the first cycle, and a superior cycle life with capacities close to 100 $mAh\,g^{-1}$ for 1000 cycles and coulomb efficiencies > 99.87 %. A one-to-one comparison with the analogue lithium-based cell shows that the sodium-based system performs better and also withstands higher currents.*

The discussion on critical resources and the need for electrochemical storage technologies has recently triggered renewed interest in sodium-ion batteries as possible complements to the well-established lithium-ion technology, especially for stationary energy stores. A considerable number of potentially interesting compounds has been identified and discovered within the last few years.[1–6] However, the search for electrode materials with sufficient cycle lives is in its infancy, especially with respect to anode materials. Although very similar cell reactions can at first sight be anticipated for both battery systems, the difference in the ionic radii between sodium and lithium leads to changes in the thermodynamic and kinetic properties, which might be advantageous or disadvantageous with respect to a reversible cell reaction. The differences in the phase behavior of $LiCoO_2$ and $NaCoO_2$,[7] the discharge products of Li/O_2 and Na/O_2 cells,[8] and the solvation properties[9] are illustrative examples. Graphite is another intriguing case. It is used in most of the commercial LIBs as an anode material because of its ability to reversibly intercalate lithium by forming a series of binary graphite intercalation compounds (*b*-GIC) with the final stoichiometry LiC_6.[10,11] Although the alkali metals K, Cs, and Rb are also known to form *b*-GICs, sodium is a notable exception. No *b*-GICs exist under moderate conditions, which is assumed to be the result of an unfavorable mismatch between the graphite structure and the size of the Na ion.[12,13] Thus, to date, it is commonly accepted that graphite unfortunately cannot be used as an electrode material for sodium-ion batteries.

Herein we report the opposite and show that graphite can be used effectively as an electrode material for NIBs exhibiting excellent reversibility at low overpotentials and superior cycle life. For this, we make use of the formation of ternary GICs (*t*-GICs),[14] that is, the intercalation of solvated alkali ions ("co-intercalation") by reduction of graphite according to Equation (1),

$$C_n + e^- + A^+ + y\,solv \rightleftharpoons A^+(solv)_yC^-_n \quad (1)$$

with C_n being *n* carbon atoms of the graphite lattice, A^+ an alkali metal, and solv a solvent molecule.[15] The chemical formation of this kind of GICs is a well-known phenomenon and early reports date back to the 1950s ($Na(NH_3)_2C_{12}$)[16] and 1960s ($Li(HMPA)C_{32}$, $Na(HMPA)C_{27}$),[17] for example. Later on, electrochemical methods were also applied to prepare a variety of *t*-GICs.[18–20] Most attention was paid to the alkali metals Li and K and the solvents dimethyl sulfoxide (DMSO), dimethoxyethane (DME), propylene carbonate (PC), and ethylene carbonate (EC). We note that the chemistry of binary and ternary GICs is very rich in general, that is, is not restricted to only alkali ions. Anions (graphite shows a redox-amphoteric behavior) and large ions can also be intercalated.[10,11,19–23] In the special case of sodium, this means that co-intercalating solvent molecules can resolve the otherwise unfavorable size mismatch between sodium ions and the graphite lattice.

It is important to know for the following that co-intercalation of solvent molecules is highly undesired in LIBs as the *t*-GICs are unstable with respect to solvent reduction, that is, the co-intercalated solvent molecules decompose, thereby leading to exfoliation of the graphite electrode and hence poor cycle life.[24–27] At low potentials, the *t*-GICs also becomes unstable with respect to the binary GICs Li_xC_n. The reason why graphite can be used in LIBs is due to the fortunate coincidence that the decomposition of EC leads to a particularly favorable solid electrolyte interphase (SEI) between the graphite and electrolyte that prevents further co-intercalation.[28] By contrast, we find that the formation of a *t*-GIC with the composition $A(diglyme)_yC_n$ (A = Li, Na) is surprisingly reversible, and in the case of sodium exhibits very favorable electrode properties. To the best of our knowledge,

[*] M. Sc. B. Jache, Dr. P. Adelhelm
Institute of Physical Chemistry, Justus-Liebig-University Giessen
Heinrich-Buff-Ring 58, 35392 Giessen (Germany)
E-mail: philipp.adelhelm@phys.chemie.uni-giessen.de

[**] We acknowledge support within the LOEWE program of excellence of the Federal State of Hessen (project initiative STORE-E). We thank Jürgen Janek, Siegfried Schindler, and Martin Winter for valuable discussions and Imerys (Bodio, Switzerland) for providing graphite materials.

Supporting information for this article is available on the WWW under http://dx.doi.org/10.1002/anie.201403734.

co-intercalation of solvent molecules for use in Na-ion batteries and studies on the prolonged cycling behavior have not been reported previously in the literature.

Figure 1 shows that the intercalation process is strongly affected by the type of solvent. The standard electrolyte used in LIBs is based on a blend of EC/DMC and $LiPF_6$ as conductive salt.[25] In this electrolyte, the *b*-GIC LiC_6 is reversibly formed at potentials below 0.25 V with a theoretical capacity of $q_{th} = 372\ mAh\,g^{-1}$.[28] As no such binary sodium GIC exists, the achievable capacities are virtually zero in the case of the analogue sodium cell (Figure 1 a,b). By using a single-solvent electrolyte based on diglyme and lithium (LiOTf) or sodium triflate (NaOTf) as the conductive salt, the electrochemical behavior changes significantly (Figure 1 a,c,d). In both cases, capacities around 90–100 $mAh\,g^{-1}$ within the first ten cycles are found. Several steps can be observed in the voltage profile, which are indicative of more complex ordering phenomena with different thermodynamic stabilities. The initial irreversible capacities are small, with values around 10–15 $mAh\,g^{-1}$, and stable capacity values are quickly reached. Notably, the overpotentials depend on the state of the discharge/charge and are much smaller for the sodium cell (typically smaller than 100 mV) than for the lithium cell (> 250 mV), together with a more stable cycle life. In particular, the kinetic limitation is negligible for the last intercalation step below 0.5 V versus Na/Na^+. Results from electrochemical impedance spectroscopy support this finding (see Figure S2 in the Supporting Information). The higher average intercalation potentials compared to the formation of LiC_6 in EC/DMC are a strong indication of *t*-GIC formation, as co-intercalation generally leads to a shift of the intercalation plateau to higher voltages.[18,25,29–31]

Very similar characteristics are found by cyclic voltammetry (Figure 2 and see Figure S2 in the Supporting Information). The voltammograms show several peaks, indicative of a series of thermodynamically defined structures that subsequently evolve during discharge and charge.[19] It can be further seen that the sodium cell exhibits a much better cycling stability than the analogous lithium system. Notably, the lithium cell does not show any redox behavior at higher cycle numbers (it is shown below that this is due to the high peak current densities occurring during the cyclic voltammetric experiment that lead to rapid degradation of the electrode). To verify that no undesired side reactions contribute to the assumed cell reaction, a series of reference experiments were conducted by testing the electrochemical stability of the current collectors and using different types of graphite and conducting salts (see Figures S3–S5 in the Supporting Information). Furthermore, the electrochemical stability of the electrolyte towards oxidation was determined to exceed 4.4 V versus Na/Na^+ (see Figure S6 in the Supporting Information).

In conclusion, the formation of a *t*-GIC is the only feasible explanation for the observed redox behavior. Notably, for the lithium cell, an additional current signal appears at low potentials which might be due to partial reductive decomposition of the solvent, combined with the formation of the binary Li-GICs. Of course, this reaction is irreversible and, therefore, is one probable reason for the observed poor cycle

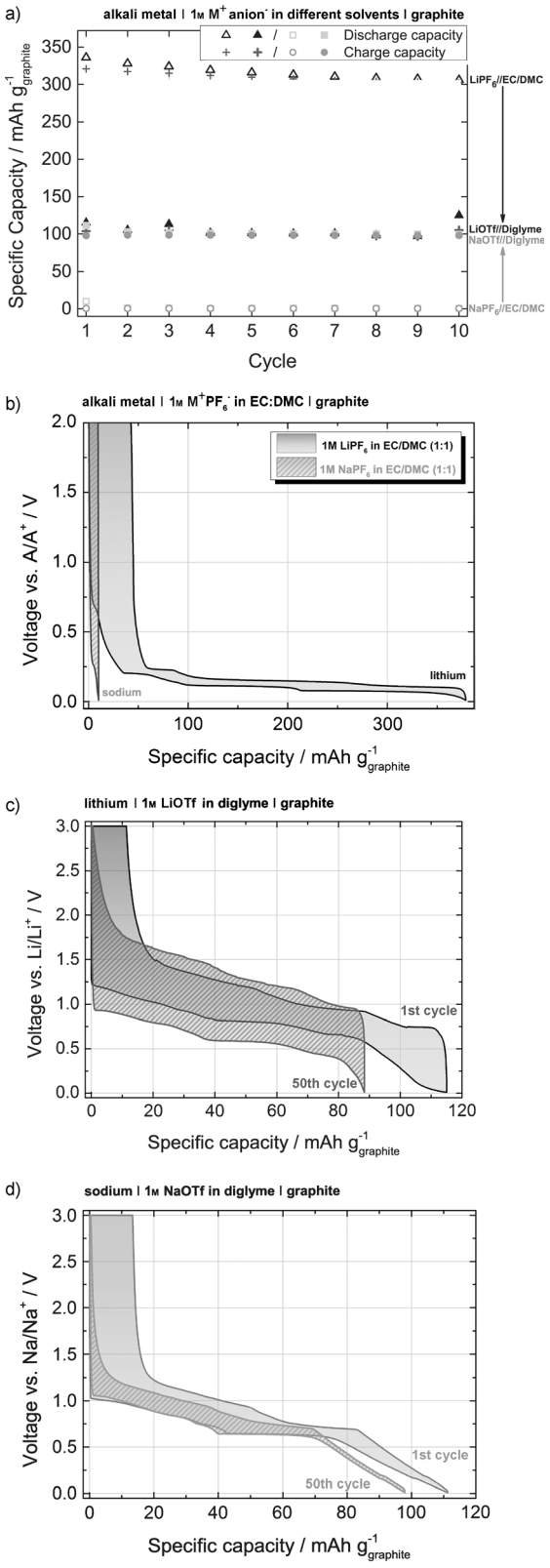

Figure 1. Specific capacities and charge/discharge characteristics of lithium/graphite and sodium/graphite cells cycled at $i = 37.2\ mA\,g^{-1}$ in different electrolytes. a) 1 M $M^+(PF_6)^-$ in EC/DMC and 1 M $M^+(OTf)^-$ in diglyme; b) 1 M $M^+(PF_6)^-$ in EC/DMC; c,d) 1 M $M^+(OTf)^-$ in diglyme. Note that the redox activity of the cells is given versus Li/Li^+ and Na/Na^+, respectively.

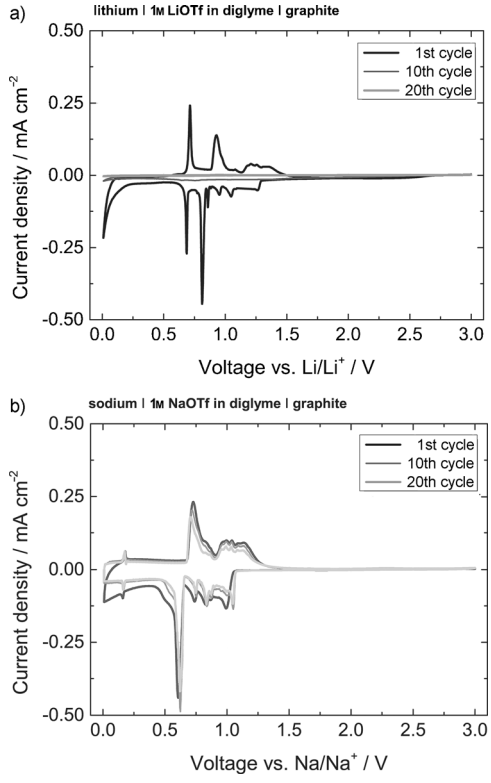

Figure 2. Redox behavior followed by cyclic voltammetry (sweep rate 0.05 $mV s^{-1}$ between 0.01 and 3.0 V).

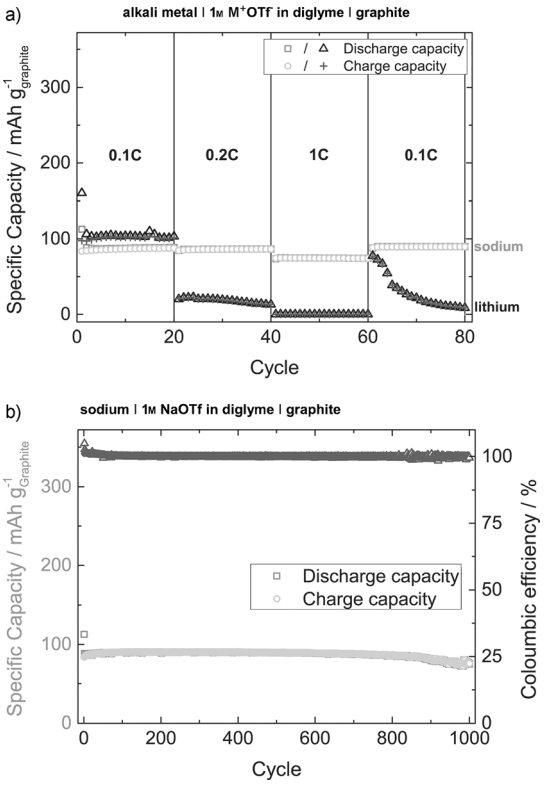

Figure 3. a) Specific capacities of lithium/graphite and sodium/graphite cells cycled at different C rates (1 C = 372 $mA g^{-1}$). b) Cycle stability and coulombic efficiency of the sodium/graphite cell in 1 M NaOTf in diglyme over 1000 cycles at 0.1 C (corresponding voltage profiles are shown in Figures S7 and S8 in the Supporting Information).

life. For sodium, this additional peak is much smaller and the cycle life is not affected. A second reason for the observed poor cycle life in the case of lithium can be discerned from Figure 3a. This graph shows the effect of current density (1 C = 372 $mA g^{-1}$) on the capacity and cycle life. Here, the sodium cell shows a significantly better performance. The obtained capacity values are quite close to the maximum value at all the applied current densities, thus indicating good kinetic properties and a mechanically stable electrode. The lithium cells can only be cycled at low currents with the maximum capacity and rapid fading occurs once the electrode has been exposed to higher currents. Current densities exceeding 0.1 C (37.2 $mA g^{-1}$) are in the same range as the maximum areal peak current densities observed in the voltammograms (0.45 $mA cm^{-2}$ corresponds to 155 $mA g^{-1}$), hence electrode degradation as a result of poor kinetic properties is a second plausible degradation mechanism of the lithium cells. A very important observation is that the sodium cell shows superior cycle life (Figure 3b). A thousand cycles were obtained with coulombic efficiencies > 99.87 % and the overpotentials remained small for several hundred cycles (see Figure S8 in the Supporting Information).

X-ray diffraction was used to study the intercalation process from a structural perspective. An expansion of the distance between adjacent graphite layers is expected during the intercalation of intercalants into the graphite host material.[10,11,16,32] In the case of reversible intercalation, a reversible shift of the (002) diffraction line to lower scattering angles occurs. The larger the increase in the layer distance, the larger the shift. Additionally, a diffraction line at higher scattering angles emerges.

These features can be clearly seen in Figure 4 (the measured values and the calculated graphite layer distances are shown in Table S1 in the Supporting Information and support reversible intercalation processes in both cells). A 10 % expansion for lithium intercalation and a 15 % expansion for sodium was found. We further used a coin cell equipped with an X-ray transparent window for a first quasi in situ study following the changes in the diffraction pattern during cell discharge (see Figure S10 in the Supporting Information).

It can be concluded from the equations derived by Rüdorff and Dresselhaus[10,16,33] for the identity period that in both cases a stage-1 intercalation compound was formed, that is, the intercalant layers are separated by one graphite layer (see Table S1 in the Supporting Information). Resolving the exact geometric alignment of the co-intercalated solvent molecules between the graphite layers and the stoichiometry with respect to the alkali ions is more difficult to determine. At least for the latter aspect, a reasonable prediction can be made. Henderson and Rhodes et al. studied the crystalline phases of several glyme:AX compounds (A = Li^+, Na^+; X = anions) and found that the alkali ions are preferentially coordinated by six oxygen atoms.[34,35] As diglyme possesses three ether oxygen atoms, two molecules would be necessary

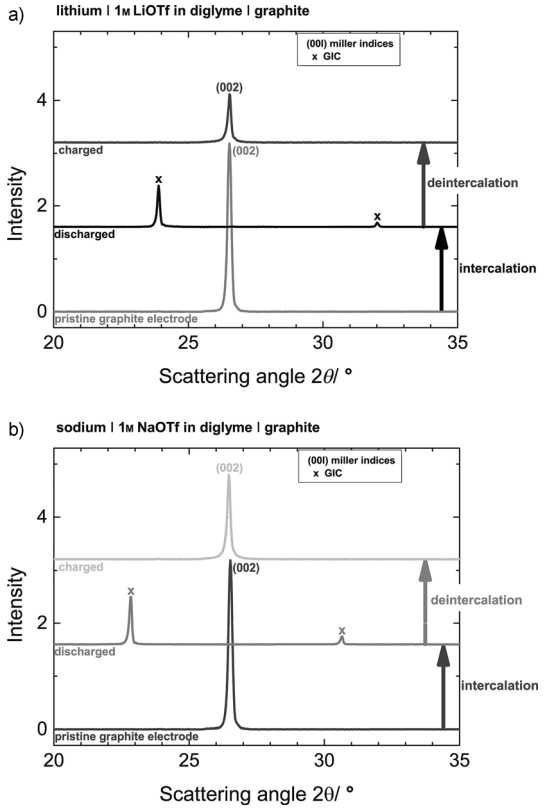

Figure 4. Diffraction patterns of the graphite electrodes for a) the lithium and b) the sodium cell. Bottom: pristine graphite electrode, middle: discharged to 0.01 V versus Li or Na (after three and a half cycles), top: charged to 3.0 V (a survey diffraction pattern (10–80°) is shown in Figure S9 in the Supporting Information). All patterns were normalized to the highest reflex of the copper current collector (Miller index (200)). Kapton tape was used to protect the samples from air.

to reach a stable solvation shell in dilute solution. As the ions approach the electrode surface, the solvation shell is deformed and the coordination number usually decreases. However, theoretical studies by Matsui and Takeyama on diglyme-solvated Li ions showed that the solvation shell still consists of two diglyme molecules even in the vicinity of the electrode.[36] It might, therefore, be reasonable to assume that two diglyme molecules are co-intercalated per alkali ion. Further studies to prove this assumption experimentally are planned. As the maximum achievable capacity value is around 100 $mAh\,g^{-1}$—corresponding to around 20 carbon atoms per intercalant—the final composition of the *t*-GICs formed in our experiments can be described as: Li-$(diglyme)_yC_{20}$ and Na$(diglyme)_yC_{20}$, with $y=1$ or more likely 2 (see Table S2 in the Supporting Information). Based on these assumptions, approximately 200 μL of solvent per gram of graphite are probably co-intercalated (see Table S3 in the Supporting Information).

In summary, we have demonstrated that graphite, in contrast to the general view, can be used as an electrode material in NIBs by taking advantage of the formation of ternary GICs. The important features of this electrode reaction are the small irreversible capacity, the low overpotentials, and the superior cycle life. The exceptional stability might be simply related to the fact that binary GICs between sodium and graphite do not form. With a capacity close to 100 $mAh\,g^{-1}$, the electrode is attractive for stationary applications. Furthermore, only relatively low cost substances were used for this study. As *t*-GICs are also formed with other solvents, our results suggest an alternative route to search for new electrode reactions for NIBs.

Experimental Section

Electrode slurries were made from as-received graphite powder (SFG-44, TIMCAL Graphite), polyvinylidene fluoride (PVDF Solef 1013, Solvay), and *N*-methyl-2-pyrrolidone (NMP, Sigma Aldrich). The content of graphite and binder was 90 wt% and 10 wt%, respectively. Electrodes were prepared by doctor blading a slurry onto copper foil ($d=10$ μm). The thicknesses of the electrodes were approximately around 40–50 μm in the dried state. Circular electrodes ($d=1.2$ cm) were punched out and contained 4–5 mg active mass each. These were further dried at 120 °C for 2 h under vacuum to evaporate residual NMP and then transferred into an argon-filled glove box (GS Glovebox System Technik), where three-electrode Swagelok type cells for cyclic voltammetry and two electrode coin cells (CR2032, MTI Corporation) for galvanostatic cycling were assembled. Lithium foil (Rockwood Lithium) or sodium (BASF) was used as the counter and reference electrodes. Whatman glass microfiber filters (GF/A) were used as separators. A commercially available 1M solution of $LiPF_6$ in 1:1 w/w EC/DMC (LP30, Selecti-Lyte, Merck) and a self-made electrolyte containing 1M $NaPF_6$ (purity > 99.0%, Alfa Asear) in 1:1 w/w EC/DMC (purity > 99.0%, Sigma Aldrich) were used as the electrolytes. Furthermore, two single-solvent electrolytes based on diglyme (purity > 99.5%, Sigma Aldrich) with 1M LiOTf (> 99.995%, Sigma Aldrich) or NaOTf (purity > 98.0%, Acros) were prepared. Electrochemical measurements were conducted at 25 °C in a climate cabinet using a Maccor battery cycler (Model 4300). Cells were cycled galvanostatically (constant current) at different C rates between 0.01 V and 3.0 V. All potentials reported herein were measured against the lithium or sodium metallic counter electrode. For comparison with the Li-ion technology, the C rate was calculated based on the theoretical capacity of graphite ($Q=372\,mAh\,g^{-1}$, that is, formation of LiC_6), thus 1 C corresponds to a current of $i=372\,mA\,g^{-1}$. Capacities are given in mAh per gram of graphite ($mAh\,g^{-1}$(graphite)). Furthermore, cyclic voltammetry was conducted (Biologic VMP3) with a voltage sweep rate of $0.05\,mV\,s^{-1}$ for at least 10 cycles. WAXS diffraction patterns were recorded with a PANanalytical EMPYREAN (Cu-Kα source, 40 kV, 40 mA) in a 2θ angular range between 10° and 80° under a protective self-adhesive Kapton foil (VWR) to avoid exposure of the sample to air.

Received: March 27, 2014
Published online: July 23, 2014

Keywords: electrochemistry · graphite · sodium

[1] H. Pan, Y.-S. Hu, L. Chen, *Energy Environ. Sci.* **2013**, *6*, 2338–2360.
[2] S. W. Kim, D. H. Seo, X. H. Ma, G. Ceder, K. Kang, *Adv. Energy Mater.* **2012**, *2*, 710–721.
[3] B. L. Ellis, L. F. Nazar, *Curr. Opin. Solid State Mater. Sci.* **2012**, *16*, 168–177.
[4] V. Palomares, M. Casas-Cabanas, E. Castilllo-Martinez, M. H. Han, T. Rojo, *Energy Environ. Sci.* **2013**, *6*, 2312–2337.
[5] M. D. Slater, D. Kim, E. Lee, C. S. Johnson, *Adv. Funct. Mater.* **2013**, *23*, 947–958.

[6] F. Klein, B. Jache, A. Bhide, P. Adelhelm, *Phys. Chem. Chem. Phys.* **2013**, *15*, 15876 – 15887.
[7] R. Berthelot, D. Carlier, C. Delmas, *Nat. Mater.* **2011**, *10*, 74 – 80.
[8] P. Hartmann, C. L. Bender, M. Vračar, A. K. Dürr, A. Garsuch, J. Janek, P. Adelhelm, *Nat. Mater.* **2013**, *12*, 228 – 232.
[9] D. Monti, E. Jónsson, M. R. Palacín, P. Johansson, *J. Power Sources* **2014**, *245*, 630 – 636.
[10] M. S. Dresselhaus, G. Dresselhaus in *Advances in Physics*, Taylor And Francis, London, **1981**, pp. 139 – 326.
[11] G. Schmuelling, T. Placke, R. Kloepsch, O. Fromm, H.-W. Meyer, S. Passerini, M. Winter, *J. Power Sources* **2013**, *239*, 563 – 571.
[12] J. Sangster, *J. Phase Equilib. Diffus.* **2007**, *28*, 571 – 579.
[13] K. Nobuhara, H. Nakayama, M. Nose, S. Nakanishi, H. Iba, *J. Power Sources* **2013**, *243*, 585 – 587.
[14] H.-P. Boehm, R. Setton, E. Stumpp, *Pure Appl. Chem.* **1994**, *66*, 1893 – 1901.
[15] J. O. Besenhard, H. P. Fritz, *Angew. Chem.* **1983**, *95*, 954 – 980; *Angew. Chem. Int. Ed. Engl.* **1983**, *22*, 950 – 975.
[16] W. Rüdorff, E. Schulze, *Z. Anorg. Allg. Chem.* **1954**, *277*, 156 – 171.
[17] D. Ginderow, R. Setton, *Carbon* **1968**, *6*, 81 – 83.
[18] J. O. Besenhard, *Carbon* **1976**, *14*, 111 – 115.
[19] P. Schoderböck, H. Boehm, *Synth. Met.* **1991**, *44*, 239 – 246.
[20] T. Abe, N. Kawabata, Y. Mizutani, M. Inaba, Z. Ogumi, *J. Electrochem. Soc.* **2003**, *150*, A257 – A261.
[21] Y. Mizutani, T. Abe, M. Inaba, Z. Ogumi, *Synth. Met.* **2002**, *125*, 153 – 159.
[22] O. Tanaike, M. Inagaki, *Synth. Met.* **1998**, *96*, 109 – 116.
[23] M. Inagaki, O. Tanaike, *Carbon* **2001**, *39*, 1083 – 1090.
[24] W. Schalkwijk, B. Scrosati in *Adv. Lithium-Ion Batter.*, Kluwer Academic/Plenum Publishers, New York, **2002**, pp. 40 – 47.
[25] K. Xu, *Chem. Rev.* **2004**, *104*, 4303 – 4417.
[26] D. Aurbach, E. Granot, *Electrochim. Acta* **1997**, *42*, 697 – 718.
[27] S. Tobishima, H. Morimoto, M. Aoki, Y. Saito, T. Inose, T. Fukumoto, T. Kuryu, *Electrochim. Acta* **2004**, *49*, 979 – 987.
[28] M. Winter, J. O. Besenhard, M. E. Spahr, P. Novak, *Adv. Mater.* **1998**, *10*, 725 – 763.
[29] M. Winter, J. O. Besenhard in *Handbook of Battery Materials*, Wiley-VCH, Weinheim, **2011**, pp. 433 – 478.
[30] J. O. Besenhard, H. P. Fritz, *Electroanal. Chem. Interfacial Electrochem.* **1974**, *53*, 329 – 333.
[31] J. O. Besenhard, H. Möhwald, J. J. Nickl, *Carbon* **1980**, *18*, 399 – 405.
[32] X. Zhang, N. Sukpirom, M. M. Lerner, *Mater. Res. Bull.* **1998**, *34*, 363 – 372.
[33] W. Rüdorff, *Angew. Chem.* **1959**, *71*, 487 – 491.
[34] W. A. Henderson, *J. Phys. Chem. B* **2006**, *110*, 13177 – 13183.
[35] C. P. Rhodes, M. Khan, R. Frech, *J. Phys. Chem. B* **2002**, *106*, 10330 – 10337.
[36] T. Matsui, K. Takeyama, *Electrochim. Acta* **1998**, *43*, 1355 – 1360.

